High frequency impedance spectroscopy analysis of doped PZT ceramics

S.B. BALMUS*, N. HORCHIDAN[a], S. POPESCU[b], V. CIUPINA[b]
Department of Sciences, Al. I. Cuza Univ., 11 Bv. Carol I, 700506 Iasi, Romania
[a] *Department of Physics, Al. I. Cuza Univ., 11 Bv. Carol I, 700506 Iasi, Romania*
[b]*Department of Physics, Ovidius Univ., Bv. Mamaia no.124, 900527, Constanta, Romania*

An impedance spectroscopy method was employed for the determination of radiofrequency (RF) and microwaves (MW) dielectric characteristics of co-doped dense PZT ceramics. The particular behavior of the cylindrical ceramic samples, i.e. the "self-resonances" were observed and analyzed. In order to have a simple and clear explanation of the RF and MW sample resonances, a dielectric resonant cavity model was developed and used. The PZT samples were considered as dielectric resonant cylindrical cavities characterized by the resonance frequency f_{r1} for the fundamental TM_{110} mode and f_{r2} for the TM_{210} resonance mode, which were observed experimentally in the frequency range of *100 MHz – 1 GHz*. The simplified theoretical approach, the particular case of the frequencies shifts for different positions of the samples inside the measurement head of the Agilent E4991A RF Impedance/Material Analyzer and the comparison between the calculated and measured data, for both low and high frequencies, are presented. The specified material analyzer is designed to work properly in certain permittivity - frequency domains, for samples having the dimensions closed to the measuring head's electrodes diameter [1]. Getting out from these requirements, as for higher then 500 relative permittivity materials and for frequencies higher then 100 MHz, induces big errors on the directly measured values of the permittivity and permeability. Evaluating the resonance frequencies of high permittivity ceramic samples considered as dielectric resonant cavities is very useful in determination of the "true" value of the effective complex permittivity of a given material, in measurements as Impedance Spectroscopy, Frequency Domain Reflectomery FDR and Time Domain Reflectomery TDR. The paper also presents a detailed model for calculating the needed corrections, starting with the high frequencies data obtained by using the specified Impedance/Material Analyzer and the low frequencies data obtained by using the SOLATRON 1260A system, the condition of continuity at 1 MHz and the high frequencies resonances of the doped PZT samples.

(Received September 8, 2011; accepted April 11, 2012)

Keywords: High frequency impedance spectroscopy, Dielectric resonant cavity model, PZT ceramics samples, High permittivity materials, Self resonances of the cylindrical samples.

1. Introduction

Because of the increasing demand on using high permittivity materials in the radiofrequency (RF) and microwave (MW) range, the electric characteristics of these dielectrics should be carefully investigated in the mentioned frequency domains. Also the existing measurement methods for usual dielectric materials should be improved and new ones developed. The main goal of this paper is to offer an analysis of the dielectric behavior of $PbZr,TiO_3$ (PZT) doped with Sr, Sb and Mn ceramic samples and also to present the particularities of the permittivity measurement technique used for this samples. We present: low and high frequency electrical characteristics of the mentioned materials, the particular self resonances (oscillation modes) of the sample behavior for high permittivity PZT ceramics in RF and MW range, the dielectric resonant cavity model, the resonance frequencies shifts for different positions of the sample inside the measurement head of Agilent E4991A RF Impedance/Material Analyzer and a comparison between the calculated and measured data, for both low and high frequencies.

Also it is presented a detailed model for calculating the needed corrections, starting with: the high frequencies data obtained by using the specified Impedance/Material Analyzer and the low frequencies data obtained by using the SOLATRON 1260A system, the condition of continuity at 1 MHz and the high frequencies resonances of the doped PZT samples. These resonance modes (frequency and quality factor) depend on the sample geometric shape and dimensions, on the equivalent permittivity of the material of the sample and on the electromagnetic field configuration which excite the sample. In order to have a simple and clear explanation of the RF and MW samples resonances, the dielectric resonant cavity model was developed. The PZT samples are considered as dielectric resonant cylindrical cavities characterized by the f_{r1} resonance frequency for the fundamental TM_{110} mode and by f_{r2} for the TM_{210} resonance mode, which were experimentally observed in the frequency range of *100 MHz – 1 GHz*. These self-resonances of the samples were experimentally obtained, by using the same measurement tecnique, for many others high permittivity materials (e.g. BT, BST, doped PZT and PZTN) in the same mentioned frequency domain. In other papers the self resonances of the samples were wrongly considered by some authors as: intrinsic relaxations of the material [2], negative

permittivity domains materials [3] or were partially explained by complicated self-inductances and self-capacitances [4] and other models [5].

2. Dielectric characterization

It was studied a doped PZT series of dielectric ceramic samples, with different percents (1%, 2%, 3%, 4%) of added PbO to stoichiometric PZT (stoichiometric PZT = PZT doped with Sr, Sb and Mn), obtained by sintering at 1330 ^{o}C. For both low and high frequencies cases, the measured samples are high density disks (cylinders with the radius around 8.66 mm and the thickness between 1.3 and 1.6 mm) with metallic thin layers on the plane surfaces.

2.1. Low frequencies dielectric characterization

The dielectric characteristics of PZT ceramics with lead excess at low frequencies (0 – 10^6 Hz) were measured by using the SOLATRON 1260A system. The real part of relative permittivity dependencies on low frequency for the mention PZT samples series are presented in Fig. 1 a, b, c.

The relative real part of permittivity depends on added PbO content and it slowly decreases in the frequency range of 10^0-10^6 Hz, for all the compositions (Fig. 1a). All the permittivity values rank between 850-940 in this frequency domain and the highest values are obtained for the stoichiometric material (Fig. 1b). The piezoelectric effects occur for all samples in the 10^4 – 10^6 Hz frequency domain. Also it is important to notice that the values of the relative real part of permittivity of the PZT series samples, obtained by measurements using the SOLATRON 1260A system, around 1 MHz, are between 870 and 900. In sections 3.2 and 3.3, these values will be used for validating the proposed "cylindrical dielectric resonant cavity model" for the samples and, by comparison with the ones obtained around 1 MHz with the Agilent E4991A RF Impedance/Material Analyzer, for calculating the corrections needed for the determination of "true value" of the permittivities at high frequency (10^6 – 10^9 Hz). These corrections are necessary because the diameters of the PZT samples are bigger then the diameter of the electrodes of the measuring head of the Agilent E4991A RF Impedance/Material Analyzer and because the permittivity-frequencies domains correlation requirements, mentioned in the analyzer's user manual [1], are not satisfied. So, the permittivity values directly provided by this device are affected by big errors and they are not the "true" ones.

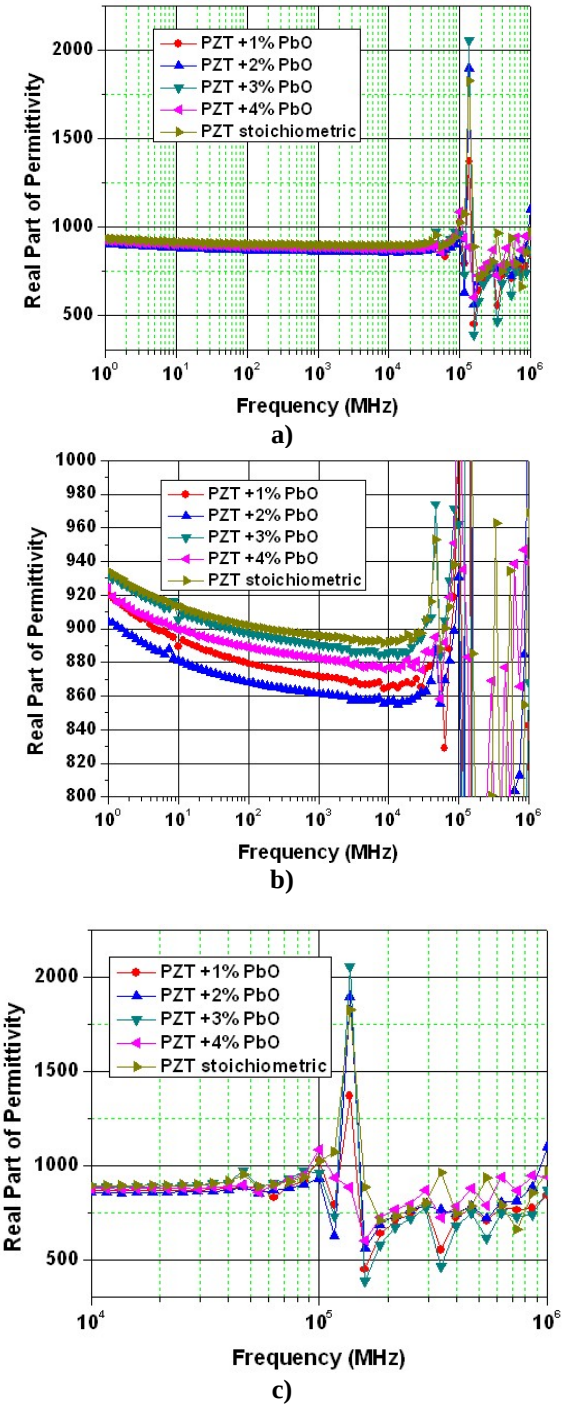

Fig. 1. Real part of the permittivity dependencies: a - for f = 10^0-10^6 Hz; b - details for f = 10^4-10^6 Hz; c - zoom for f = 10^0-10^6 Hz

The imaginary part of relative permittivity dependencies on low frequency for the mention PZT samples series are presented in Fig. 2 a, b, c.

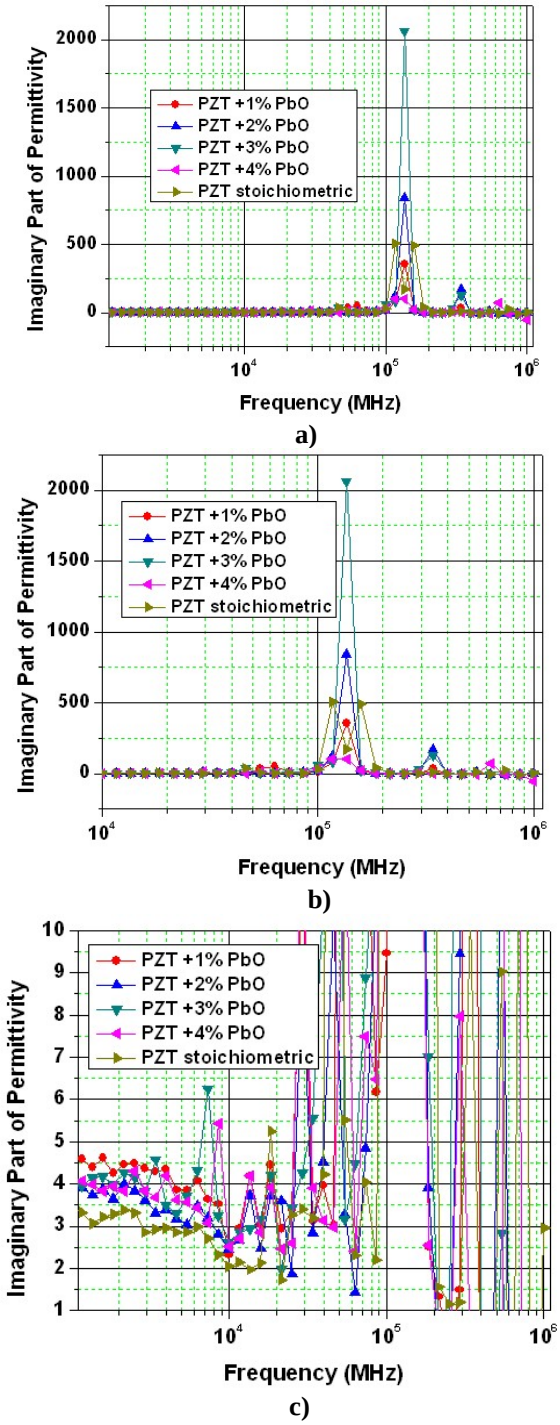

Fig. 2 Imaginary part of the permittivity dependencies: a - for f = 10^0-10^6 Hz; b - details for f = 10^4-10^6 Hz; c - zoom for f = 10^0-10^6 Hz

The imaginary part of the relative permittivity increases when PbO is added in different percents. The same piezoelectric effects occur for all samples in the 10^4 – 10^6 Hz frequency domain.

2.2. High frequencies dielectric characterization

The permittivity measurements at high frequency (10^6 – 10^9 Hz) were performed using the Agilent E4991A RF Impedance/Material Analyzer. The measuring head's electrodes have the diameter of 7 mm which is smaller than the sample diameters.

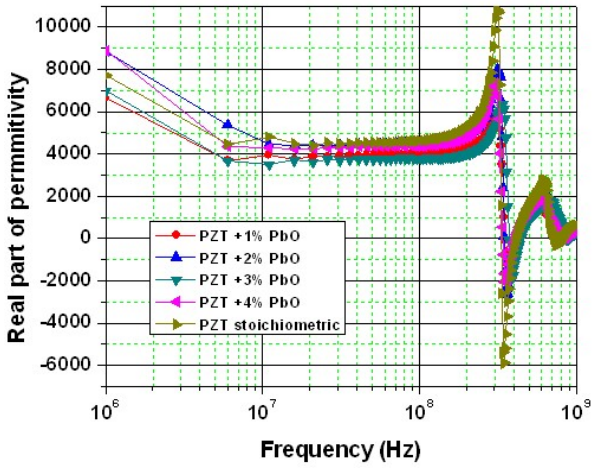

Fig. 3. Real part of the directly measured permittivity dependencies for f = 10^6-10^9 Hz

The relative permittivity dependencies on high frequency for the mention PZT series samples are presented in Figs. 3, 4, 5 and 6. It could be remarked the decrease of the real part and the increase of imaginary part of the relative permittivity of the samples, when PbO is added in different percents and also two regions, around 3.5×10^8 and 6.5×10^8 Hz**,** in which the real permittivity presents resonance shapes and the imaginary permittivity presents absorption shapes. It is important to remark the negative values of the real permittivity and also that the resonances shift to higher frequencies when the real permittivity is decreased by the addition of PbO which means that resonance frequencies are proportional with the inverse of the real permittivity. The first important question is how to explain these resonances: their resonance frequencies, their shifts and the negative values of the real permittivity?

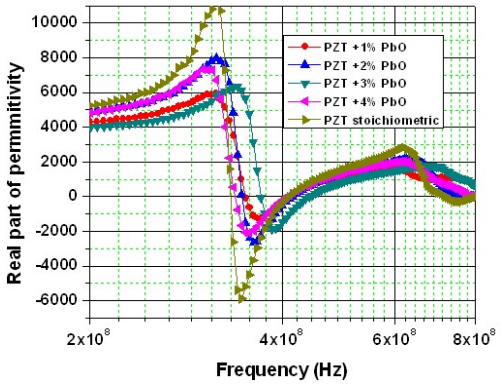

Fig. 4. Zoom on the real part of the directly measured permittivity dependencies for f = 2×10^8-8×10^8 Hz

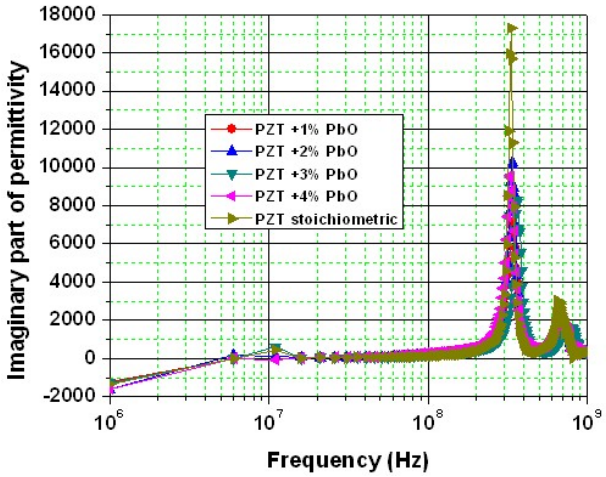

Fig. 5. Imaginary part of the directly measured permittivity dependencies for $f = 10^6$-10^9 Hz

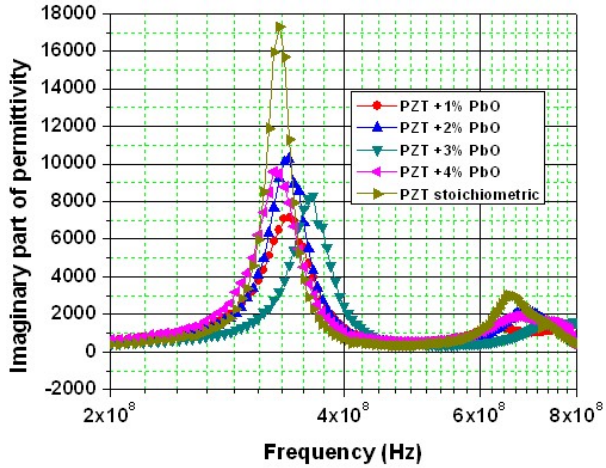

Fig. 6. Zoom on the imaginary part of the directly measured permittivity dependencies for $f = 2\times10^8$-8×10^8 Hz.

It is important to notice that the values of the real permittivity, obtained by directly measurements with the Agilent E4991A RF Impedance/Material Analyzer around 1 MHz are situated between 3500 and 4500 and that they are totally different from the ones measured at low frequency with the SOLATRON 1260A system, at the same frequency. So, the continuity condition for the real part of permittivity at 1 MHz, by taking into account the directly measured data, it is not accomplished. From this fact derives the second important question: Which are the "true" values of the real part and imaginary part of permittivity at high frequency? We recall here that the mentioned analyzer is designed to work properly in certain permittivity - frequency domains, for samples having the diameter close to the measuring head's electrodes diameter [1]. Getting out from these requirements, as for higher then 500 relative permittivity materials and for frequencies higher then 100 MHz, induces big errors on the directly measured values of the permittivity and permeability.

In table 2.1 are presented the experimental data directly obtained from measurements by using the SOLATRON 1260A system and also the Agilent E4991A RF Impedance/Material Analyzer around 1 MHz.

Table 1 Experimental real permittivity comparison around 1 MHz

Sample	Real permittivity measured by the SOLATRON 1260A system	Real permittivity measured by the Agilent E4991A RF Analyzer
PZT	892	4500
PZT +1% PbO	866	3900
PZT +2% PbO	857	4400
PZT +3% PbO	886	3700
PZT +4% PbO	877	4300

Another important question is how to explain why the resonances frequencies shift when the samples are placed in different positions inside the measuring head of the Agilent E4991A RF Impedance/Material Analyzer. In Fig. 7 are presented the experimental real permittivity data directly obtained by measurements when the same stoichiometric PZT sample is place in different positions inside the measurement head: in the centre, 1mm, 2 mm and 3 mm backside.

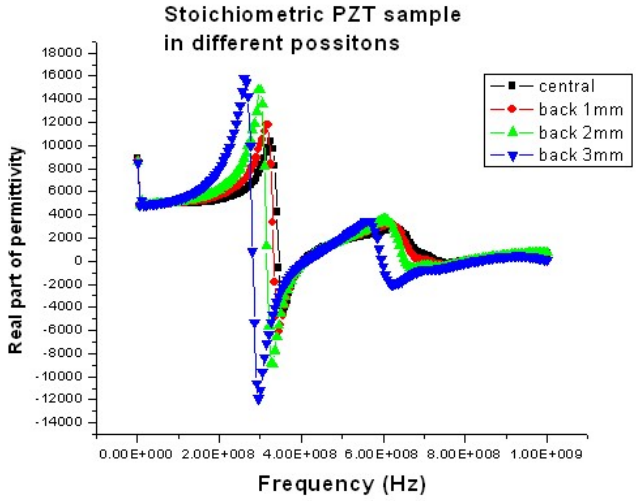

Fig. 7. Stoichiometric PZT sample in different positions inside the measuring head of the E4991A RF Analyzer.

The answers for these three very important questions are given in sections 3.2 and 3.3, by using a "cylindrical dielectric resonant cavity model" for explaining the resonances and to determine of the needed corrections for the high frequency permittivity calculus.

3. Cylindrical dielectric resonant cavity model and data interpretation

The PZT samples with lead excess are considered as dielectric resonant cylindrical cavities characterized by the f_{r1} resonance frequency for the fundamental TM_{110} mode and by f_{r2} for the TM_{210} resonance mode.

In this section are presented the theoretical "cylindrical

dielectric resonant cavity" model proposed by us for the samples, the validation of this model by resonance frequencies calculus and comparison with the experimental data. Also the true values of the real permittivity at high frequencies obtained by using the mentioned model and the needed corrections are presented.

3.1. Cylindrical dielectric resonant cavity theoretical model

3.1.1 Simple dielectric cylinder (disk)

A simple dielectric cylinder represents a resonant cavity, in which appear TE or/and TM resonance (oscillation) modes when it is excited by an incident electromagnetic field, depending on the incident field configuration or on the cavity excitation method. In Fig. 8 is presented the dielectric resonant cavity characterized by the height *L*, radius *a* and ε_r dielectric constant [6].

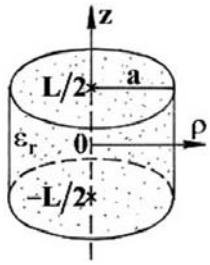

Fig. 8 Cylindrical dielectric resonator.

Starting with the oscillation equation and using PMW (Perfect Magnetic Wall) boundary condition at the dielectric – air interfaces, the characteristics (field configuration, resonance frequency and quality factor) of the oscillation modes are obtained. For the approach used in this paper the resonance frequencies are very important. So, the resonance frequencies are given by [6]

$$f_{r,nmp} = \frac{c_0}{2\pi\varepsilon_r^{1/2}\mu_r^{1/2}}\left[\left(\frac{\rho_{nm}}{a}\right)^2 + \left(\frac{p\pi}{L}\right)^2\right]^{1/2} \tag{1}$$

for the TE_{nmp} modes and

$$f_{r,nmp} = \frac{c_0}{2\pi\varepsilon_r^{1/2}\mu_r^{1/2}}\left[\left(\frac{\rho'_{nm}}{a}\right)^2 + \left(\frac{p\pi}{L}\right)^2\right]^{1/2} \tag{2}$$

for the TM_{nmp} modes, where:
- *a* is the radius of the cavity
- c_0 is the electromagnetic waves velocity in free space
- ε_r is the relative real part of the permittivity
- μ_r is the relative real part of the permeability
- ρ_{nm} is the "m^{th}" solution of the *first* kind and "*n*" order "J_n" Bessel function
- ρ'_{nm} is the "m^{th}" solution of the "J'_n" derivative
- *p* is an integer number: $p = 0,1,2,...$ for the TE_{nmp} and $p = 1,2,3,...$ for the TM_{nmp} modes

The modes characterized by the lowest resonance frequencies are called the fundamental oscillation modes and their resonance frequencies are given by [6]

$$f_{r,010} = \frac{c_0\rho_{01}}{2\pi a\varepsilon_r^{1/2}\mu_r^{1/2}} = \frac{2.405}{2\pi\varepsilon_r^{1/2}\mu_r^{1/2}a}c_0 \tag{3}$$

for the TE_{010} fundamental mode and

$$f_{r,111} = \frac{c_0}{2\pi\varepsilon_r^{1/2}\mu_r^{1/2}}\left[\left(\frac{\rho'_{11}}{a}\right)^2 + \left(\frac{\pi}{L}\right)^2\right]^{1/2} = \frac{c_0}{2\pi\varepsilon_r^{1/2}\mu_r^{1/2}}\left[\left(\frac{1.841}{a}\right)^2 + \left(\frac{\pi}{L}\right)^2\right]^{1/2} \tag{4}$$

for the TM_{111} fundamental mode.

3.1.2. Thin dielectric cylindrical sample with thin metal layers on the plane (flat) surfaces

For this kind of resonant dielectric cylindrical cavities (also the case of the measured PZT ceramics with lead excess) the resonance modes are obtained by applying PEW (Perfect Electric Wall) boundary conditions on the metal – dielectric plane (flat) interfaces and PMW (Perfect Magnetic Wall) boundary conditions on the circular dielectric – air interface.

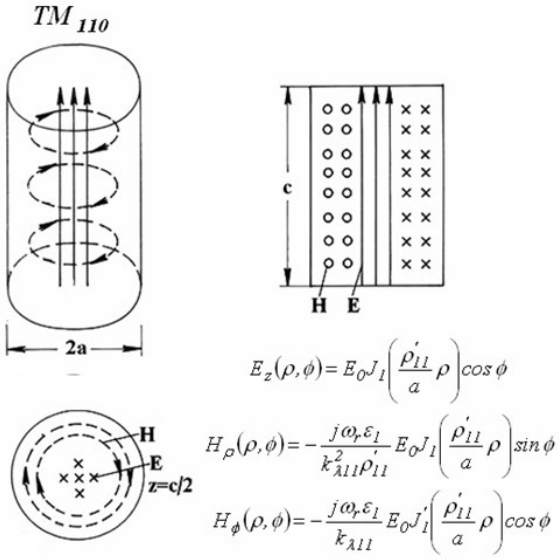

Fig. 9. Theoretical TM_{110} electromagnetic field configuration inside the sample [6].

For thin dielectric cavities, when their heights are smaller than the wavelength of the electromagnetic field

which excites the sample, appear also the TM_{nm0} modes *(p=0 - uniform electromagnetic field configuration along z axis).* By taking into account the electric field configurations, orientated along z axis, which is also created by the measuring head's electrodes it was concluded that only the TM modes could be excited in the sample. For the approach used in this paper only the first two, the fundamental TM_{110} and TM_{210} resonance modes, were taken into account and are next characterized.

In Fig. 9 are presented the TM_{110} spatial electromagnetic field configuration, longitudinal and transversal cuts and also the mathematical expressions of the fields.

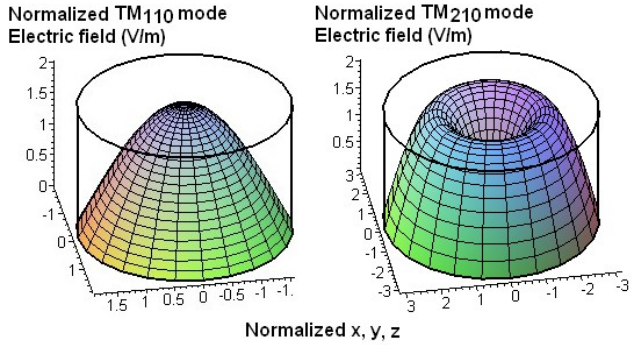

Fig. 10. Theoretical normalized TM_{110} and TM_{210} electric field configuration inside the sample

In Fig. 10 we can be observed the differences between the electric field configuration for the TM_{110} mode, which present its maximum along the symmetry axis of the cylindrical sample, and the TM_{210} mode which presents a minimum along the symmetry axis of the cylindrical sample and its maximum at the half of the radius. The electromagnetic field configurations for these two mentioned resonance modes are uniform along z axis.
The resonance frequencies are:

$$f_{r1} = \frac{c_0 \rho'_{11}}{2\pi a \varepsilon_{eff}^{1/2}} = \frac{1.841}{2\pi \varepsilon_{eff}^{1/2} a} c_0 \qquad (5)$$

for the fundamental TM_{110} mode and

$$f_{r2} = \frac{c_0 \rho'_{21}}{2\pi a \varepsilon_{eff}^{1/2}} = \frac{3.054}{2\pi \varepsilon_{eff}^{1/2} a} c_0 \qquad (6)$$

for the TM_{210} resonance mode, where ε_{eff} is the effective relative real part of dielectric permittivity and $\mu_r = 1$.

3.2. Experimental and theoretical data comparison

In Fig 11 could be observed the characteristics of the measurement head, the uniform electric field configuration in the free space between the two electrodes of the measurement head (without the sample) and the TM_{110} Bessel dependence of the electric field configuration in the interior of the cylindrical samples.

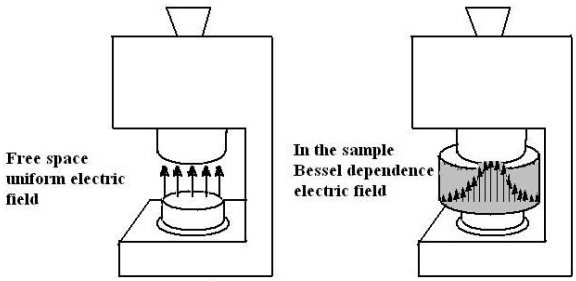

Fig. 11. Measurement head and the TM_{110} electric field configuration inside the sample.

In Table 2 is presented a comparison between the theoretical frequencies obtained by calculus (Eq. 5 and Eq. 6) for TM_{110} and TM_{210} resonance modes, by taking into account the real permittivity values given by the SOLATRON 1260A system around 1 MHz, and the experimental resonance frequencies obtained by measurements.

Table 2. Theoretical and experimental resonance frequencies comparison

Sample	Radius (mm)	Experimental relative real permittivity at 1 MHZ	TM110 theoretical frequency (MHZ)	TM110 experimental frequency (MHZ)	TM210 theoretical frequency (MHZ)	TM210 experimental frequency (MHZ)
PZT	8.65	892	340.42141	330	564.71862	655
PZTN 1% PbO	8.66	866	345.09492	340	572.47141	680
PZTN 2% PbO	8.63	857	348.10815	340	577.47001	685
PZTN 3% PbO	8.65	886	341.57213	365	566.62754	676
PZTN 4% PbO	8.74	877	339.78497	325	563.66285	670

By taking into account the very good concordance of theoretical and experimental resonance frequencies for the TM_{110} resonance mode, with a maximum relative error of 3 - 5 %, and the similitude between the electric field configuration created by the electrodes of the measuring head and the *TM* modes electric field configuration inside de samples, it is clear that these first resonances around 3.5×10^8 Hz are well explained by the TM_{110} resonance mode. The bigger differences of 10 - 15 % between the second resonances around 6.5×10^8 Hz and the TM_{210} resonance modes are explained by the fact that, for this frequency range, the real permittivity is lower then the one from 1 MHz (the real permittivity decreases with frequency [7]).

Eq. 5 and eq. 6 explain also the shifts of the resonances when the permittivity is decreased by the addition of PbO. By decreasing the real permittivity, which appears in both formulas at the denominator, the resonances frequencies increase and vice versa.

The dielectric resonant cavity model explains also the negative permittivity domain: the effective permittivity is obtained from the signal reflected or transmitted, depending on the technique, by the sample which acts like a cavity, absorbing and emitting energy, and so, the signal obtained from the sample is positive (bigger) or negative (smaller) then the incident signal.

The shift of the resonances frequencies when the same sample is placed in different positions inside the measuring head of the Agilent E4991A RF Impedance/Material Analyzer is explained by the fact that the sample, consider as cylindrical dielectric resonant cavity, it is asymmetrically excited [8-10].

3.3. "True" values of the permittivity at high frequencies. Correction coefficients

Starting from the experimental resonance frequencies and the following formulas

$$\varepsilon_{eff} = \left(\frac{c_0 \rho'_{11}}{2\pi a f_{r1}} \right)^2 = \left(\frac{1.841}{2\pi a f_{r1}} c_0 \right)^2 \quad (5)$$

for the fundamental TM_{110} mode and

$$\varepsilon_{eff} = \left(\frac{c_0 \rho'_{21}}{2\pi a f_{r2}} \right)^2 = \left(\frac{3.054}{2\pi a f_{r2}} c_0 \right)^2 \quad (6)$$

for the TM_{210} resonance mode, the true values of the real permittivity at high frequency were calculated and they are presented in table 3.

Table 3. "True" values of the real permittivity at high frequencies in the resonance regions.

Sample	Experimental relative real permittivity at 1 MHz	TM110 calculated relative permittivity at 300 - 400 MHz	TM210 calculated relative permittivity at 600 - 700 MHz
PZT	892	949.22836	663.05029
PZTN 1% PbO	866	892.14856	613.77286
PZTN 2% PbO	857	898.362	609.05786
PZTN 3% PbO	886	775.91269	622.49473
PZTN 4% PbO	877	958.60836	620.71011

By looking in Table 4 it can be observed that the experimental data presented in the second column measured with the SOLATRON 1260A system around 1 MHz and the third column data, calculated from the experimental TM_{110} resonance frequency obtained with the E4991A RF Impedance/Material Analyzer, are in good concordance and so the continuity of real permittivity at 1 MHz is well accomplished.

Taking into account the values of the permittivity at 10^8 Hz directly measured by the E4991A RF Impedance/Material Analyzer and the true values of the permittivity calculated for the TM_{110} mode the correction coefficients were calculated and they are presented in Table 4.

Table 4. Correction coefficients.

Sample	Experimental relative real permittivity at 100 MHz	TM110 calculated relative permittivity at 300 - 400 MHz	Correction coeffients
PZT	4500	949.23	0.21
PZTN 1% PbO	3900	892.15	0.23
PZTN 2% PbO	4400	898.36	0.20
PZTN 3% PbO	3700	775.91	0.21
PZTN 4% PbO	4300	958.61	0.22

The experimental data directly measured with the E4991A RF Impedance/Material Analyzer were corrected by multiplication with these correction coefficients and the resulting data are presented in figure 12 and 13.

Of course, the values of the relative permittivity in the resonances regions are not the ones from these graphics, but the ones calculated and presented in Table 3 for the real part of permittivity and those resulting from removing the "absorption peaks" for the imaginary part of permittivity.

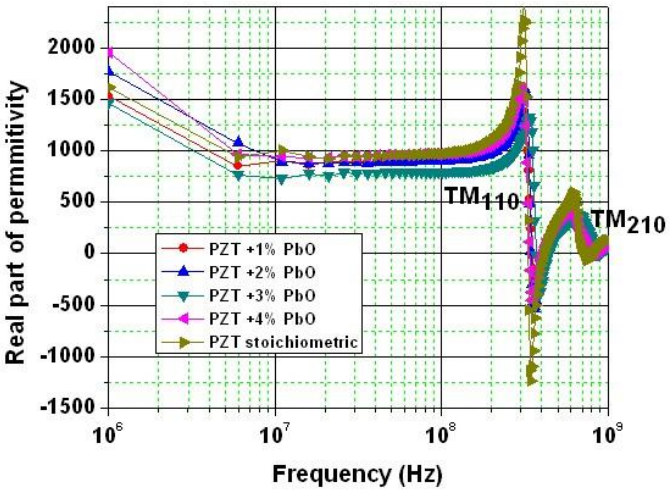

Fig. 12. True values of the relative real permittivity at high frequency

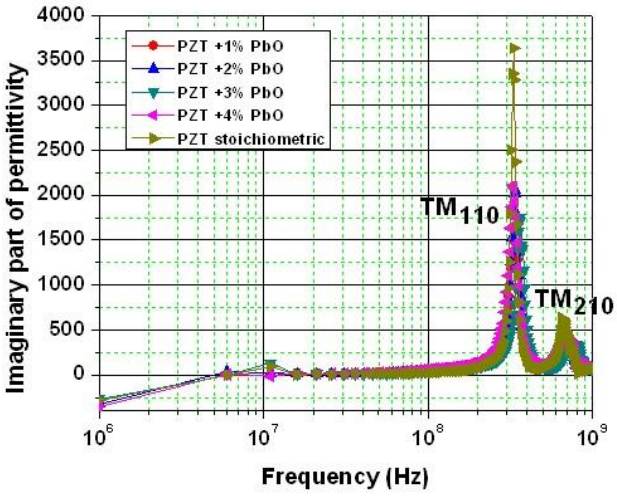

Fig. 13. True values of the relative imaginary permittivity at high frequency

5. Comments and discussions

Correctly explaining the samples resonances it is very important from the scientific, from the existing measurement methods and from the utilization of the new high permittivity materials for RF and Microwave devices points of view. The "cylindrical dielectric resonant cavity" model, proposed by us for the samples, explain simply and clearly these resonances.

The self resonances of the samples are used by us, in improving the existing measurement methods such as: Impedance Spectroscopy, Frequency Domain Reflectomery FDR and Time Domain Reflectomery TDR for the determination of the "true" value of the equivalent effective complex permittivity of a given material, mostly if the sample dimensions are different then the measuring head's electrodes diameter or the permittivity-frequencies domains correlation requirements, mentioned in the analyzer's user manual [1], are not satisfied, and therefore, corrections are needed.

Also, the self resonances of the samples could be used for the development of new measurement methods for the electrical properties determination of the high permittivity materials.

Acknowledgements

This work was performed by the financial support of the POSDRU/89/1.5/S/49944 Project and the POSDRU/88/1.5/S/56668 Project.

References

[1] Agilent E4991A RF Impedance/Material Analyzer Data Sheet – User Manual, Agilent Technologies, Inc. 2003, 2004, 2009, Printed in USA, March 25, 2009, 5980-1233E
[2] Mark P. McNeal, Sei-Joo Jang, Robert E. Newnham, Journal of Applied Physics, **83**(6), 15 (1998).
[3] F. Xu et al., J. Phys. D: Appl. Phys. **42**, 025403 (2009).
[4] Hirofumi Kakemoto, Jianyong Li, Song Min Nam, Satoshi Wada And Takaaki Tsurumi, Jpn. J. Appl. Phys. Vol. 42 (2003).
[5] V. Dobrincu, S.B. Balmuş, G.N. Pascariu, D.D. Sandu J. Optoelectron. Adv. Mater. **8**(3), 956 (2006).
[6] D. D. Sandu "Microwaves. Physical principles" (in romanian), VICTOR Publishing. House, Bucharest, 2005.
[7] A. Jonscher, "Dielectric relaxation in solids", Chelsea Dielectric Press, London, (1983)
[8] D.M. Pozar „Microwave Engineering", Addison Wesley Publ.Company, N.Y., (1990, reprinted 1996)
[9] R.E. Collin „Field Theory of Guided Waves", sec. edition, Oxford University Press, (1991)
[10] G. Dôme „RF Systems. Waveguides and Cavities" in AIP Conference Proceedings 153, (M. Month and M. Dienes, editors) vol 2, N.Y. (1987)

*Corresponding author: sorin.balmus@uaic.ro